Summer 1987

Mechanical and neutronic properties of neutron absorbing materials

Donald James Buth

Department:

MECHANICAL AND NEUTRONIC PROPERTIES OF NEUTRON ABSORBING MATERIALS

BY

DONALD JAMES BUTH, 1963-

A THESIS

Presented to the Faculty of the Graduate School of the

UNIVERSITY OF MISSOURI-ROLLA

In Partial Fulfillment of the Requirements for the Degree

MASTER OF SCIENCE IN NUCLEAR ENGINEERING

1987

Approved by

Albert E. Bolon (Advisor) D. Ray Edwards

Con T. May

PUBLICATION THESIS OPTION

This thesis has been prepared in the style utilized by Nuclear Technology. Pages 1 - 43 will be presented for publication in that journal. Appendices A - E have been added for purposes normal to thesis writing.

ABSTRACT

The primary neutron absorbing material examined in this project was Boraflex™, which consists of a silicone polymer with boron carbide acting as the neutron absorber. Two aluminum based neutron absorbers, Boral™ and Al-B-Ten, were also examined. Both X-ray and neutron radiography were used to examine the Boraflex™. The neutron radiography gave better resolution in detecting fluctuations in the boron carbide distribution; however, X-ray radiography did perform better in detecting flaws in the base material. Tensile tests were performed to determine the uniformity of Boraflex™'s tensile properties. The average tensile strength was calculated to be 303 ± 15 psi. A small angular dependence was found in the material; however, the tensile properties were uniform as a whole. Neutron activation analysis was used to identify the presence of trace impurities in the Boraflex™ that could become radioactive after long exposures to neutrons. The elements identified were magnesium, manganese, zinc, dysprosium, and lanthanum. The total removal cross section for thermal neutrons, and the absorption cross sections were also determined. The total cross section for Boraflex™ was 14 ± 1 barn. This was compared to Boral™, which had a cross section of 220 ± 20 barn. The absorption cross section for the Boraflex™ was 12 ± 1 barn. This value was compared to the absorption cross section of Al-B-Ten, which was 4.8 ± 0.5 barn.

ACKNOWLEDGMENTS

The author would like to thank all of the staff members at the University of Missouri-Rolla Reactor Facility for their assistance in conducting the neutron attenuation and trace element analysis experiments, and to Don Alger and Dave Peeler for their help with the neutron radiographs performed at the Missouri University Research Reactor.

Special thanks are extended to my committee members, Dr. Albert Bolon, Dr. D. R. Edwards, and Prof. R. V. Wolf for their help in conducting these experiments.

The author is grateful for the Boraflex™ and Al-B-Ten™ materials that were supplied by BISCO Industrial Services, Inc. He is also grateful for the financial support he received as a United States Department of Interior Fellow and as a Power Fellow.

And many thanks to my wife, Lisa, who has given me support and encouragement throughout this research.

TABLE OF CONTENTS

Page

LIST OF TABLES

I. INTRODUCTION

This research involved the examination of various properties of a material called Boraflex™, and the comparison of some of these properties, when possible, to other neutron absorbing materials. Boraflex™ is a composite shielding material for neutrons that is currently being used in high density fuel storage racks. It is made by adding boron carbide (B_4C) powder to a silicone polymer [1]. After the polymer solidifies it is cut into sheets and then clad in stainless steel to form the storage racks.

Boron carbide is used as a neutron absorbing material for many reasons. It contains approximately 80 atomic percent natural boron, which has two isotopes ^{10}B (18.8%) and ^{11}B (81.2%). The ^{10}B has a very high neutron absorption cross section (3836 barns) for thermal neutrons. Because of this, the B_4C also has a large cross section for thermal neutrons. Other properties that make B_4C very attractive are its hardness (Knoop Hardness Number 27.5 GPa), high melting point (2350 ^{o}C), and chemical inertness. However, B_4C performs poorly under loading because it has a relatively low tensile strength, and is very brittle [2].

Since the 1940's this problem has been avoided by combining the B_4C, in a powdered state, with other more ductile materials [3] to give a composite material that has better mechanical characteristics, while still retaining the neutronic properties of the B_4C. Aluminum, steel, polymers,

and various resins have all been used successfully for this purpose [1-7]. This paper reports the results of a study to determine the mechanical and neutronic properties of a polymer based neutron absorber, and compares the neutronic properties with some aluminum based neutron absorbers. More information on high density fuel storage racks and some of the alternate materials discussed in this report are presented in articles by Weeks [8], Burn [9], Macmillan [10], Evans [11], Judd [12], and the Electric Power Research Institute [13].

II. EXPERIMENTAL METHODS AND MATERIALS

A. OVERVIEW

The principle material that was examined in this research was Boraflex™. It is produced by BISCO Products, Inc. for use in high density fuel storage racks, and in other neutron shielding applications. The main characteristics that were examined were the B_4C distribution, the uniformity of the tensile properties, the impurity content, and the absorption and total thermal neutron cross sections. The experimental cross sections were also compared to the total cross section for Boral™, and the absorption cross section of a new absorbing material, called Al-B-Ten™, that consists of B_4C in aluminum.

B. TEST MATERIALS

Three materials were examined in this report. The primary material was Boraflex™. It is a composite material consisting of powdered B_4C in a methylated polysiloxane elastomer matrix. The material has a total thickness of 0.078 inches, and a boron loading of 0.020 g/cm^2 ^{10}B.

Boral™, a product of Brooks and Perkins Advanced Structures, was used as a reference material because of its widespread use as a neutron absorbing material. It is made by mixing powdered B_4C with approximately 50% of the required aluminum powder and then combining this mixture with molten aluminum. This mixture is then cast as ingots

and sprayed with aluminum to ensure that no B_4C is exposed. A 0.125 inch sheet of 2S aluminum is then wrapped around the material for cladding, and it is rolled, while still warm, to give a final thickness of either 0.25 or 0.125 inches [5,6]. The Boral^{TM} used for these experiments was 0.25 inches thick with a cladding thickness of 0.020 inches [6], and a ^{10}B loading of 0.101 g/cm^2.

The third material that was examined was Al-B-Ten^{TM}. It is a mixture of 40 volume percent B_4C in aluminum which is then sandwiched between two layers of pure aluminum that are approximately 5 to 10 mils thick. It has a total ^{10}B loading of approximately 0.03 g/cm^2 and a plate thickness of 0.10 inches [14].

C. RADIOGRAPHY

Both neutron and X-ray radiography were used to determine the B_4C distribution in the polymer. Both of these techniques use a source of radiation to pass through an object and then strike a film, which produces a negative image of the original object on the film. For the neutron radiography either a direct conversion or a transfer method is normally used. In the direct conversion method the neutrons pass through the object and then strike a conversion screen. This screen gives off low energy X-rays, which then expose the film. For the transfer method, the neutrons pass through the object and activate a metallic plate. This radioactive plate is then placed in contact with a piece of

film for a certain length of time in order to expose the film. This method is especially useful for radiographing radioactive materials. For X-ray radiography, the X-rays directly expose the film so that no conversion screen or transfer plate is required. However, intensifying screens are sometimes used to either give a better resolution at the same exposure, or to limit the exposure needed to give a certain film density. Each of these methods have some definite advantages and disadvantages over the other one; however, a best technique does not always exist. In many cases both techniques can be used to supplement the information from the other.

1. Neutron Radiography The first technique examined, neutron radiography, can be very useful in differentiating between two elements with similar atomic numbers, as long as the materials have a difference in their absorption cross sections. Also, neutron radiography can be used to identify flaws in a material that is encased in a metal shroud. This characteristic allows materials to be examined even after they have been clad in steel or lead. The disadvantages for the neutron radiography are that the process can be very expensive, especially if long exposure times are required, the material examined may become radioactive for a period of time, and there are not many neutron radiographic facilities available [15,16,17].

The neutron radiographs were made using the neutron

radiographic facility located on the thermal column of the Missouri University Research Reactor (MURR) at Columbia, Missouri. The beam characteristics for these radiographs include a thermal flux of $6.2*10^7$ n/cm^2s, a collimator length to diameter ratio of 38.83, and a gamma dose rate of 1.2 mR/s [14]. A 12.5 micron gadolinium conversion screen and M5 Kodak Industriex film was used to produce the radiographs through direct thermal neutron radiography. Samples 2, 6, 10, and 14 were attached to the front of a loaded 356mm by 432mm vacuum film cassette holder, which was then inserted into the sample chamber. The film was exposed to the neutrons for 1.5 hours before being removed to be processed using chemicals and procedures shown in reference 15. The finished radiographs were analyzed using a Macbeth TD-504 densitometer, and a kodak color densitometer.

2. <u>X-ray Radiography</u> The other method used to examine the Boraflex™ was X-ray radiography. X-Ray radiography has been used for non-destructive examination of many different materials since the early 1900's [17]. Because of this, there are many places available which can perform X-ray radiography at relatively low costs. The main disadvantages with X-ray radiography are its poor ability to distinguish between elements with very close atomic numbers, and its inability to radiograph objects that are radioactive.

The X-ray radiographs were made using a Faxitron X-ray machine with a tube to object distance of 25.5 inches.

Samples 2, 6, 10, and 14 were used, after they had been checked for any induced radioactivity, so that any artifacts found by either examination method could be compared with the other technique. A tube voltage of 20 kilovolts was used with an exposure of 1.25 mA-minutes. Dupont NDT 75 radiographic film was used with a 0.01 inch lead intensifying screen. The radiographs were developed using a 5-10-15 developing technique using Kodak GBX chemicals. This technique consist of a 5 minute immersion in developer followed by a 10 minute immersion in a fixer solution and ending with a 15 minute water wash. Because the samples were larger than the available film, each sample had to be radiographed in halves. This required two radiographs to be made for each sample, but by using external reference marks, the location of any artifact could be identified. The radiographs were analyzed using a Kodak Model 1 color densitometer.

D. TENSILE PROPERTIES

Tensile tests were performed on Boraflex^{TM} samples in both pre- and post-irradiated conditions. These tests were designed to determine the uniformity of the tensile properties of the Boraflex^{TM}, and to determine if these properties were isotropic. Samples were also tested to see if a small stress raiser would greatly affect the tensile properties. For these tests ASTM E-21 was followed as closely as possible, with the major difference being that

the size of the tensile specimen used was smaller than the one recommended. This procedure determined the engineering stress and percent elongation by using short term static loading. The engineering stress is defined by the equation

$$\text{Stress} = F / A_o \qquad \text{(Eq. 1.)}$$

and the percent elongation is given by

$$\% \text{ Elongation} = (l - l_o) / l_o \qquad \text{(Eq. 2.)}$$

where F is the applied load

A_o is the original cross sectional area

l is the final gage length

l_o is the original gage length

The stress raiser was a small cut in the neck of the sample. This cut was perpendicular to the length of the tensile specimen and reduced the width of the neck by 0.1 cm. It was utilized because of the difficulty involved in detecting cuts in the Boraflex^{TM} with either of the radiographic techniques, or through visual inspection. This induced stress raiser is not in accordance with the ASTM procedure being used; however, it should not adversely affect the validity of the test results since stress raisers mainly influence fatigue tests [19].

To determine if the Boraflex^{TM} had an angular dependence in its tensile properties, it was decided to perform

tensile tests on specimens that were at 0^{o}, 45^{o}, 90^{o}, and 135^{o} from the normal direction of the Boraflex^{TM} sheet. Straps 2, 3, 5, 6, 7, 9, 11, 13, and 15 were used for the unirradiated samples. Each of these straps was then subdivided into five regions, with each of the first four regions having two tensile specimens at one of the four angles. One specimen from each pair was then cut, with a razor blade knife, to create the stress raiser. The specimens were then tested on an Instron tensile machine, at the Graduate Center for Materials Research located on the University of Missouri-Rolla campus.

It was decided to give twelve other specimens a low dose of gamma radiation before any tensile tests were performed on them. These samples were taken from sections 1c, 4b, 8a, 8b, 12d, and 16c. Only 0^{o} and 90^{o} samples were used in this part of the experiment. Each of these specimens had also been exposed to a low fluence of neutrons in the attenuation experiment; however, the neutron exposure was of such a low magnitude (< 200 n/cm^{2}) that it was not expected to influence the results. To irradiate the samples, they were placed in a water tight plastic vial and lowered next to the reactor whenever it was shutdown. Care was taken to ensure that the samples were not exposed to any additional neutrons, so that they would not become activated. After the specimens had received approximately 5.1 MR of gamma radiation, they were removed from the pool and checked for any induced radiation on a lithium drifted germanium,

Ge(Li), detector. These samples were then tested on the Instron tensile machine.

E. TRACE ELEMENT DETERMINATION

Neutron activation analysis (NAA) is a very accurate method of identifying very small levels of impurities in a given base material without having to first use expensive chemical separation techniques [20]. The basic principle behind NAA is that an unknown material is exposed to a flux of neutrons. This causes each isotope in the material to be transformed to a new different isotope. Some of these new isotopes are radioactive, and they will give off their characteristic radiation. By placing this material on a high resolution detector, which is connected to a multichannel analyzer (MCA), an energy spectrum is able to be collected that contains the characteristic gamma radiation from each of the radioactive isotopes. This energy spectrum can then be analyzed to identify many of the isotopes that are present in the material. After the peaks are identified the average activity for each isotope can be used to calculate the mass of each element that is present in the material.

NAA is a very good technique to identify most impurities that may be present in a sample. However, there are some limitations to this method. Some isotopes have such a small cross section that they will not activate unless a very high fluence of neutrons is used. Also, even

after a radioactive isotope has been produced its half life may be so long or short that it is difficult to detect them on the counting system. Some isotopes will also be hidden because of other more radioactive peaks next to them. This problem can normally be avoided by taking several counts at various time intervals, to allow the isotopes with shorter half lives to decay away, and by looking for other energy peaks that the isotope in question may emit. The final problem is that no single detector system can detect all of the different types of radiation. To avoid this limitation, several different systems can be utilized so that all emitted radiation will be detected.

The Boraflex^{TM} was examined for trace element impurities by using neutron activation analysis. A long term irradiation was also performed on the Boraflex^{TM} to simulate a lifetime fluence of 10^{17} n cm^{-2}. Each sample was cleaned and then sealed in a plastic fingertip, which was then encapsulated in a rabbit tube vial. This vial was inserted into the core using a pneumatic tube system. After the sample was irradiated it was placed on a Ge(Li) detector which was connected to a IBM PC based multi-channel analyzer (MCA). After the spectrum was collected it was stored on a floppy disk for further analysis. This disk was transferred to a different computer where a Gaussian fit was used to determine the location of each peak. After the peaks were found, the computer calculated the centroid energy and net activity of each peak. The computer then compared this

energy spectrum to a library file to see if any of the peaks were identical. Finally the system gave reports over both the identified peaks and the unidentified peaks. These results were then checked by hand to determine if the identified peaks were possible, and to try to identify the remaining unidentified peaks.

F. NEUTRON ATTENUATION

1. Total Cross Section A total neutron cross section for thermal neutrons was found by using the transmission (or beam) technique. In this method a beam of neutrons from a reactor is allowed to pass through a sample and strike a detector so the neutrons may be counted. Next a count rate is taken without the sample in the beam. To ensure that only thermal neutrons are being counted, a thin sheet of cadmium is then placed in the neutron beam and an epi-cadmium count is taken with and without the sample present. This epi-cadmium count is a measure of the number of non-thermal neutrons that are being counted by the detector. The cadmium was chosen for this purpose because at low, or thermal, energies it has a very large absorption cross section, which suddenly drops to a much lower cross section for all higher energy levels. A transmission coefficient for thermal neutrons can then be determined using equation 3.

$$T = I / I_o \qquad \text{(Eq. 3.)}$$

where T is the thermal neutron transmission coefficient

I_o is the thermal neutron count rate with no sample in place

I is the thermal neutron count rate with the sample in place

A macroscopic total removal cross section cross section for thermal neutrons can then be calculated using equation 4 [21,22].

$$M = \ln(T) / x \qquad \text{(Eq. 4.)}$$

where M is the macroscopic total removal cross section for thermal neutrons

T is the thermal neutron transmission coefficient

x is the sample thickness

2. <u>Absorption Cross Section</u> The danger coefficient method was used to determine an absorption cross section for the Boraflex™ and the Al-B-Ten™. This method is an in-pile technique for measuring the reactivity of a sample. The absorption cross section can then be determined through some calculations, or by comparing the reactivity of the sample with that of a known standard [22].

To determine the reactivity of the sample, the reactor was started and taken to a low power level (20 W) and the

control rod heights were recorded. The sample was then carefully inserted into the core. Then, the reactor was taken back to the same power level, and the critical rod heights were recorded again. The difference in the rod heights was then related to the reactivity of the sample through the use of the reactor's rod worth curves [22,24,25]. To simplify these results, all of the shim/safety rods were kept at a constant height, so that the entire reactivity change was compensated by the regulating rod.

After the reactivity of the sample was determined two methods were used to calculate the absorption cross section. In the first method equation 5 was used to give an absolute value for the microscopic absorption cross section.

$$sig_a = 10^{21} * A_s * r_s / (m_s * f^2) \qquad \text{(Eq. 5.)}$$

where sig_a is the microscopic absorption cross section

A_s is the atomic weight of the sample

r_s is the reactivity of the sample (in deltaK/K)

m_s is the mass of the sample

f is the reactor flux at 20 W

In the second method, the absorption cross section is determined by comparing the reactivity of the sample to the reactivity of a known standard. This relative method uses equation 6 to give a final value for the sample's cross section.

$$sig_{a2} = r_2 * m_1 * sig_{a1} / (r_1 * m_2) \quad \text{(Eq. 6.)}$$

where sig_{a1} is the absorption cross section for the standard

sig_{a2} is the absorption cross section for the sample

m_1 is the mass of the standard

m_2 is the mass of the sample

r_1 is the reactivity of the standard

r_2 is the reactivity of the sample

III. RESULTS

A. RADIOGRAPHY

The radiographs were read on a Kodak Model 1 color densitometer. The following table shows the range of density values that were found across each radiograph. The error associated with each density measurement is ± 0.05 due to the difficulty of differentiating between the light intensities in the densitometer.

TABLE 1

RADIOGRAPHIC DATA FOR BORAFLEX^{TM} SAMPLES

	Specimen Number	Average Density	High Density	Low Density	Maximum Discontinuity
X-ray	2	0.56	0.59	0.52	None found
Neutron	2	0.85	0.89	0.81	0.75
X-ray	6	0.57	0.60	0.54	None found
Neutron	6	0.88	1.00	0.80	None found
X-ray	10	0.56	0.59	0.52	None found
Neutron	10	0.82	0.84	0.80	None found
X-ray	14	0.57	0.65	0.52	None found
Neutron	14	0.88	0.95	0.82	0.81

B. TENSILE PROPERTIES

The tensile properties have been placed into four groups for comparison purposes. The first group was used to determine if the different load cell affected the results. The second group contains the tensile data grouped by their original horizontal location in the sheet. The third group has the tensile data grouped according to their original vertical position in the sheet, and the last group was arranged by the angular orientation of the tensile specimens to the normal direction of the original sheet of Boraflex^{TM}.

TABLE 2

TENSILE PROPERTIES OF BORAFLEX^{TM} GROUPED BY THE LOAD CELL USED

Load Cell Number	Cross Sectional Area (in^2)	Percent Elongation	Stress At Failure (psi)
1	0.01611	56.2 ± 13	413 ± 47
1	0.01273	19.7 ± 3.6	233 ± 73
2	0.01611	56.9 ± 32	292 ± 34
2	0.01273	20.3 ± 4.4	231 ± 42

TABLE 3

TENSILE PROPERTIES OF BORAFLEX^{TM} GROUPED BY HORIZONTAL LOCATION

Strap Number	Cross Sectional Area (in^2)	Percent Elongation	Stress At Failure (psi)
2	0.01611	47.3 ± 8.7	290 ± 20
2	0.01273	17.0 ± 3.4	190 ± 46
3	0.01611	53.3 ± 17	390 ± 42
5	0.01611	56.8 ± 6.4	379 ± 110
5	0.01273	23.5 ± 3.4	268 ± 41
6	0.01611	52.8 ± 3.5	313 ± 22
6	0.01273	18.6 ± 0.4	203 ± 15
7	0.01611	60.1 ± 4.3	386 ± 81
7	0.01273	18.9 ± 2.2	202 ± 23
9	0.01611	55.9 ± 6.9	387 ± 105
9	0.01273	16.8 ± 1.1	230 ± 120
11	0.01611	85.0 ± 76	292 ± 45
11	0.01273	23.0 ± 4.1	257 ± 43
13	0.01611	51.3 ± 8.2	311 ± 40
13	0.01273	21.2 ± 2.7	240 ± 49
15	0.01611	55.3 ± 5.1	287 ± 35
15	0.01273	22.4 ± 2.4	231 ± 26

TABLE 4

TENSILE PROPERTIES OF BORAFLEX^{TM} GROUPED BY VERTICAL LOCATION

Strap Section	Cross Sectional Area (in^2)	Percent Elongation	Stress At Failure (psi)
A	0.01611	69.0 ± 57	337 ± 51
A	0.01273	18.3 ± 2.0	200 ± 35
B	0.01611	55.5 ± 9.0	382 ± 73
B	0.01273	20.5 ± 2.2	263 ± 68
C	0.01611	53.4 ± 15	360 ± 70
C	0.01273	22.0 ± 5.0	232 ± 57
D	0.01611	59.5 ± 4.3	371 ± 71
D	0.01273	19.7 ± 3.6	211 ± 42
E	0.01611	50.2 ± 6.3	269 ± 23

TABLE 5

TENSILE PROPERTIES OF BORAFLEX^{TM} GROUPED BY ANGLE OF SAMPLE

Angle Of Specimen	Cross Sectional Area (in^2)	Percent Elongation	Stress At Failure (psi)
0^o	0.01611	54.3 ± 5.2	319 ± 70
0^o	0.01273	19.6 ± 3.2	214 ± 49
45^o	0.01611	64.6 ± 49.3	337 ± 77
45^o	0.01273	21.2 ± 2.2	259 ± 68
90^o	0.01611	51.7 ± 15.4	340 ± 64
90^o	0.01273	20.8 ± 4.3	228 ± 55
135^o	0.01611	57.1 ± 5.2	382 ± 76
135^o	0.01273	19.2 ± 4.2	209 ± 40

TABLE 6

TENSILE PROPERTIES OF IRRADIATED BORAFLEX™

Cross Sectional Area (in^2)	Percent Elongation	Stress At Failure (psi)
0.01611	91.4 ± 8.8	144 ± 14

C. TRACE ELEMENT ANALYSIS

The following tables show the concentration of all of the identified isotopes in the Boraflex™. The first table identifies short term activation products, and the second table identifies long term activation products. The short term activation was performed at a thermal power of 20 kW for 10 minutes. For the long term activation, samples were lowered next to the core for four, four hour runs with the reactor at a thermal power of 200 kW, this gave each sample a neutron fluence of 6E+16.

TABLE 7

TRACE ELEMENTS IDENTIFIED IN SHORT TERM ACTIVATION OF BORAFLEX™

Isotope	Concentration (uCi/g)
Mg-27	3.16E+0 ± 1.56E-1
Mn-56	4.48E-1 ± 3.00E-2
Zn-69m	4.22E-2 ± 2.73E-3
Mo-101	2.14E+0 ± 4.02E-1
Eu-152m	1.08E-1 ± 2.43E-2
Dy-165	2.93E-1 ± 4.03E-2

TABLE 8

TRACE ELEMENTS IDENTIFIED IN LONG TERM ACTIVATION OF BORAFLEX™

Isotope	Concentration (uCi/g)
Sc-46	5.54E-4 ± 2.26E-4
Zn-69m	1.39E+0 ± 2.63E-2
La-140	3.53E-2 ± 1.32E-3

D. NEUTRON ATTENUATION

Tables 8 through 10 show the results of the total removal cross section for thermal neutrons. They contain the data for Boraflex™, Boral™, and aluminum. The aluminum was used as a benchmark for the attenuation setup. There was a 10 percent statistical error for the attenuation data for the Boraflex™ and the Boral™, while the aluminum only had a 2 percent statistical error in its measurement.

TABLE 9

TOTAL THERMAL CROSS SECTION

FOR BORAFLEX^{TM}

Thickness (inches)	Transmission Coefficient	Macroscopic Cross section (cm^{-1})	Microscopic Cross section (barns)
2.203125E-01	2.11E-02	1.79E+01	2.37E-23
4.406250E-01	1.51E-02	1.10E+00	1.46E-23
6.609375E-01	5.75E-03	7.29E+00	1.04E-23
8.812500E-01	4.91E-03	6.04E+00	8.02E-24

TABLE 10

TOTAL THERMAL CROSS SECTION

FOR BORAL^{TM}

Thickness (inches)	Transmission Coefficient	Macroscopic Cross section (cm^{-1})	Microscopic Cross section (barns)
2.500000E-01	8.83E-03	1.89E+01	2.40E-22
2.500000E-01	8.83E-03	1.89E+01	1.98E-22

TABLE 11

TOTAL THERMAL CROSS SECTION

FOR ALUMINUM

Thickness (inches)	Transmission Coefficient	Macroscopic Cross section (cm^{-1})	Microscopic Cross section (barns)
2.500000E-01	9.24E-01	3.16E-01	5.25E-25
5.000000E-01	8.55E-01	3.13E-01	5.19E-25
7.500000E-01	8.15E-01	2.73E-01	4.53E-25

Table 11 shows the calculated absorption cross sections for Boraflex™, and Al-B-Ten™. This data had a 10 percent statistical error in its initial measurement.

TABLE 12

THERMAL ABSORPTION CROSS SECTION FOR BORAFLEX™ AND AL-B-TEN™

Material	Absorption Cross Section	
	Relative (barns)	Absolute (barns)
Boraflex™	1700 ± 200	12 ± 1
Al-B-Ten™	780 ± 80	4.8 ± 0.5

IV. DISCUSSION AND ANALYSIS OF RESULTS

A. RADIOGRAPHY

The X-ray and neutron radiographs were used to determine the uniformity of the B_4C distribution in the Boraflex™. The two methods were also compared to see if any artifacts that were discovered using the one method could also be found by using the other. Data for the radiographs can be found in Table 1 and in Appendix B.

A penetrameter was made for each method so that the quality of the radiographs could be determined. The dimensions and corresponding film densities of these penetrameters can also be found in Appendix B. One problem that was found with the X-ray penetrameter was that even a single thickness of scotch tape or paper affected the film density. This was due to the low tube voltage and short exposure time used for the X-ray radiographs. However, the tape and paper were needed to have a consistent penetrameter. Because of this, the true density readings for the X-ray penetrameter were lower than the recorded values; however, the ratio of thickness change-to-density change is believed to be the same. The tape used for the neutron penetrameter is not believed to have caused any difference in the density readings because of the low cross section for the elements in the tape, and the high exposure time.

The results showed a fluctuation in the film density across both the X-ray and neutron radiographs of five

percent. These minor fluctuations could have been because of some minor variations of the B_4C distribution or some variations in the actual polymer base material. The neutron radiographs showed some places that had a noticeable decrease in the film density. This was believed to have been caused by some of the B_4C clumping together. However, no locations were found that had noticeable density increases, which would have probably corresponded to a B_4C decrease. The average densities for all of the radiographs was very close, except for the neutron radiograph of sample 10, which had an average density of 0.82 ± 0.05. This value can be compared to the average neutron radiograph density of 0.87 ± 0.05. This difference corresponded to a thickness change of only 5.6%, which was not considered to be a very significant fluctuation in B_4C density. Therefore, the Boraflex™ appears to have a very uniform B_4C distribution.

The X-ray and neutron radiographs were also compared to one another to see if any artifacts would show up in both of them. The purpose of this comparison was to determine if X-ray's could be used as either a supplement or substitute to the currently used neutron radiography. Samples 6 and 14 were chosen for this comparison because both of their neutron radiographs had noticeable decreases in their film density at a set location, and sample 14 had a 0.25 inch tear in one of its edges. No noticeable density changes were found in either of the X-ray radiographs; however, the tear was visible in the X-ray of sample 14. The neutron

radiograph for sample 14, on the other hand, did not show any evidence of the tear. This is due to the low cross section of the base material not having any effect on the radiograph. Even though a tear did exist in the material, it was not pulled apart so the B_4C loading was not affected. Also, the Boraflex^{TM} is self adhesive so it did not allow the tear to gap open, unless a load was applied. Because of this type of situation, it is suggested that both X-ray and neutron radiography should be used to examine the material for defects. The neutron radiography is the superior technique to identify fluctuations in the B_4C loading, while the X-ray radiography is better at detecting flaws in the base material. X-ray radiography could also be used to determine whether a decrease in the B_4C density was due to a void in the base material, or whether it was due to a lower concentration of B_4C in the affected area.

B. TENSILE PROPERTIES

The data for the tensile properties of the Boraflex^{TM} specimens were grouped in several manners to see what relationships, if any, existed in the material. All of the data was first sorted according to the load cell that was used by the Instron machine. The data was then sorted by the original location of the sample on the sample sheet. This included sorting by both the strap number, which was related to the original horizontal location of the specimen on the sheet, and strap section, which was related to the

original vertical location of the specimen on the sheet. The data was also grouped by angle, as measured from the normal direction of the main sheet. The irradiated samples were grouped in the same manner, with the exception that all tests were performed with the second load cell, and the only angles used were 0^{o} and 90^{o} from the normal direction of the sheet. The tensile properties of the unirradiated and irradiated samples were then compared to see if a relationship existed between any of the tensile characteristics for the material and the total gamma dose that the material had received.

From the data presented in Tables 2 through 5 and Appendix C it can be seen that no strong relationship existed between the original location of the specimen or the angle of the specimen, and its tensile properties. The best correlations were found for specimens tested at the different angles. This may be because the angular specimens were chosen from all parts of the original sheet instead of a certain horizontal or vertical location. The worst data correlation was found with the horizontally grouped data. This data had a standard deviation of 3.6% for the percent elongation and 59 psi for the tensile strength.

The average percent elongation for a smooth edged piece of material was 55 $\pm$ 2.1. This is 2.7 times higher than the average percent elongation for the cut samples, which was 20 $\pm$ 1.0. The main reason for this decrease in elongation before failure was due to the fact that the material tore

very easily, and the cut induced into the side of the specimen gave a good starting point for the tear. This tear continued to increase in length, when the load was applied, until the specimen failed because of tearing. In contrast, the uncut specimens showed some necking before they failed suddenly.

The average tensile strength at failure was 303 $\pm$ 18 psi for the uncut specimens, and 225 $\pm$ 20 psi for the cut specimens. The failure strength was not as sensitive to the condition of the specimen as the percent elongation was. The main reason for this was that once a maximum loading was reached in the uncut samples the material experienced some necking before failure, while the cut specimens failed without any noticeable necking. This absence of any necking was what allowed the ultimate tensile strengths to be relatively close while the percent elongation results had a much larger difference.

For best results, all of the tensile tests should have been performed without any changes to the tensile machine or the room environment. Between the second and third day of testing the load cell was damaged by a different researcher, which made it necessary to replace the load cell. After the load cell was replaced, the average tensile strength was found to be lower than the value determined from the earlier data. No reason exists for this difference, since the Instron machine was calibrated before each session and the room was at a relatively constant temperature. Therefore,

the data from the first two days of tests were considered to be valid, and were therefore used to calculate the average tensile properties of the Boraflex™.

The samples that received 5.1 MR of exposure to gamma rays had a percent elongation of 91.4 ± 8.8 and a tensile strength at failure of 144 ± 14 psi. This is a 52% lower tensile strength than the unirradiated samples, but a 66% higher percent elongation than the unirradiated samples. Previous tensile tests had been performed on the Boraflex™ material. The results from this previous test gave a tensile strength range of 151 to 263 psi for the unirradiated samples and a tensile strength range of 150 to 714 psi for the irradiated samples. The unirradiated results correspond well with the present results: however, a large decrease in the tensile properties was observed in this research for the irradiated samples, while the previous research reported a tensile strength increase. This discrepancy may be due to the amount of radiation the samples were exposed to. In the earlier research the samples were exposed to an average of 1.70E+10 R, while the current research was limited to 5.1E+06 R.

C. TRACE ELEMENT DETERMINATION

Neutron activation analysis was used to determine the amount of impurities in the Boraflex™. All of the identified peaks are listed in Tables 6 and 7 and in Appendix D. Some other peaks were not able to be identified, either by

hand or by the computer based nuclide library. The possibility also exists for one of the identified peaks to be obscuring a peak from a different isotope. Much care was taken to prevent this situation from occurring by taking multiple counts of each sample at many different time intervals, and using different counting time increments. The isotopes that were the most likely to be missed would have to have a very short half life. Because of this, they would not give a significant contribution to any long term induced activity in the sample.

The sodium and chlorine were probably due to salt contamination in or on the fingertip, or they were extra contaminates on the outside surface of the Boraflex™. The isotopes that have the greatest likelihood of existing in the Boraflex™ are europium, manganese, magnesium, zinc, dysprosium, and lanthanam.

D. NEUTRON ATTENUATION

A total removal cross section for thermal neutrons was determined for Boraflex™, Boral™, and aluminum. This cross section data can be found in Tables 9 and 10. The aluminum cross section was experimentally determined to serve as a benchmark value for the experimental setup.

The average aluminum cross section was calculated to be 0.499 barns. This is 2.14 times higher than the accepted value for aluminum (0.233 barns). Because of this result a correction factor of 2.14 $\pm$ 2% will be utilized to calculate

the remaining transmission cross section results.

The transmission coefficients and macroscopic cross sections are believed to be the most accurate of the cross section results. There was some question as to whether the number densities used for the microscopic cross section determination were correct. For this reason, all of the results will be expressed in terms of the macroscopic cross section with the microscopic cross section enclosed in parentheses. The calculated total thermal removal cross section for Boraflex^{TM} was determined to be 8.0 $\pm$ 0.8 cm^{-1} (14 $\pm$ 1 barn), and for Boral^{TM} it was 19 $\pm$ 2 cm^{-1} (220 $\pm$ 20 barn).

The absorption cross section was found by first determining the reactivity worth of a sample of Boraflex^{TM} and Al-B-Ten^{TM}, using the danger coefficient method. The cross section was then calculated by either a absolute or relative method. The absolute method used the reactivity worth of the sample and the thermal neutron flux at the irradiation position to calculate the absorption cross section. This method gave a value of 12 $\pm$ 1 barn for the Boraflex^{TM} and a value of 4.8 $\pm$ 0.5 barn for the Al-B-Ten^{TM}. The relative method related the reactivity change due to the unknown sample the reactivity change from a known standard. This technique gave a relative absorption cross section of 1900 $\pm$ 200 barn for the Boraflex^{TM} and 780 $\pm$ 80 barn for the Al-B-Ten^{TM}. A boron standard was not available so cadmium was chosen as the standard. Because the cadmium does not have

the same absorption characteristics as the boron, this method is not expected to give exact results for the Boraflex^{TM} and the Al-B-Ten^{TM}. However, this method did give a valid correlation factor between the absorption cross sections of Al-B-Ten^{TM} and Boraflex^{TM}. The absorption cross section of the Boraflex^{TM} was determined to be 2.48 times higher than the absorption cross section of the Al-B-Ten^{TM}.

V. CONCLUSION

This research focused on several different properties of Boraflex^{TM}. The radiographic studies showed a very uniform boron carbide distribution throughout the material. However, the neutron radiography showed an inability to detect tears in the material, which would decrease the materials ability to stretch before failing, and its tensile strength at rupture. This problem may not be serious since the Boraflex^{TM} is normally clad in stainless steel, and it does not support any load. Tears could be detected if X-ray radiography would be used in addition to the normal neutron radiography. This technique is relatively inexpensive and it would be able to detect thickness fluctuations, voids, and tears in the material.

The tensile properties were checked to determine the uniformity of the mechanical characteristics of the Boraflex^{TM}. The average tensile strength was calculated to be 303 $\pm$ 15 psi. There was a major increase in the tensile strength for samples 5, 7, and 9. These samples had an average tensile strength at rupture of 384 $\pm$ 4.6 psi. Because of this fluctuation, sample 6 was checked to see if its properties were also high. Its tensile strength was calculated to be 317 $\pm$ 3.2 psi. No reason is expressed for this increase; however, all of the high data was collected on the same day. Therefore, a calibration problem might have existed, even though the calibration was checked before

the samples were tested. Because no reason can be found to prove this data is erroneous, it was not discarded. When the angular dependence was checked, a 10% increase in tensile strength was found for the samples at 135^{o} from the normal direction to the sheet. This may be due to a preferred orientation of B_4C grains in the polymer, or even a preferred orientation for the polymer chains. However, no reason was identified for this change in tensile strength.

Twelve tensile samples were also exposed to a gamma intensity of 5.1 MR. These specimens had a percent elongation of 91.4 $\pm$ 8.8 and a tensile strength at failure of 144 $\pm$ 14 psi. This is a 52% lower tensile strength than the unirradiated samples, but a 66% higher percent elongation than the unirradiated samples. Previous tensile tests had been performed on the Boraflex^{TM} material. The results from the previous test showed an increase in tensile strength and a corresponding decrease in ductility for high levels of gamma exposure. This is the reverse of the current results. Also, some bubbles were detected on the surface of the Boraflex^{TM} after the samples were removed from the pool. Because of these results, it is suggested for intermediate range gamma exposures be performed to give a better understanding of the materials physical property changes during a pure gamma exposure.

The trace element analysis showed the presence of europium, magnesium, manganese, zinc, dysprosium, and lanthanum. Sodium and chlorine were also identified;

although, their presence was believed to have been caused by salt contamination of the plastic fingertip or the surface of the material. Some minor peaks were not identified. However, the major detectable impurities are believed to have been identified.

Both total and absorption cross sections, for thermal neutrons, were determined in this research. The average total cross section for Boraflex^{TM} was calculated to be 10 $\pm$ 1 cm^{-1} (14 $\pm$ 1 barn). This can be compared to the total cross section for Boral^{TM}, which was calculated to be 19 $\pm$ 2 cm^{-1} (220 $\pm$ 2 barn). The absorption cross section for the Boraflex^{TM} and Al-B-Ten^{TM} were calculated through both a relative and absolute method. The relative method gave an absorption cross section of 1900 $\pm$ 200 barn for Boraflex^{TM} and 780 $\pm$ 80 barn for the Al-B-Ten^{TM}. These results may not be exact values, though, because the standard sample used was cadmium, which has different absorption resonances than the boron. However, this technique was able to relate the absorption cross sections of the Al-B-Ten^{TM} to the Boraflex^{TM}. This relation showed that the absorption cross section for the Boraflex^{TM} is 2.5 $\pm$ 10% times greater than the absorption cross section for the Al-B-Ten^{TM}.

BIBLIOGRAPHY

1. J. S. Anderson, Technical Director, Boraflex Neutron Shielding Material Product Performance Data, Report 748-30-1, Brand Industrial Services, Inc. (Bisco), (August 25, 1979).

2. N. H. Macmillan, G. I. Dooher, and R. G. Naum, "The Behavior of a Boron Carbide (B_4C)-phenolic and a Glass Fiber-reinforced Boron Carbide (B_4C)-phenolic Composition in a Spent Nuclear Fuel Storage Pool," Nuclear Technology, vol. 59, pp. 327-43, (1982).

3. O. Rudiger, J. Stickforth, and G. Lohrke, "Boral as Protective Material Against Thermal Neutrons," Tech. Mitt. Krupp, Vol. 19, pp. 154-72, (Nov. 1962).

4. V. L. McKinney and T. Rockwell, III., Boral: A New Thermal Neutron Shield, Oak Ridge National Lab., (June 16, 1953).

5. B. Kopelman, Materials for Nuclear Reactors, McGraw Hill, New York, pp. 387,388 (1959).

6. W. D. Wilkinson, W. F. Murphy, Nuclear Reactor Metallurgy, D. Von Nostrand Co., Inc., New York, p. 306 (1959).

7. J. S. Anderson, Technical Director, Irradiation Study of Boraflex Neutron Shielding Materials, Report 748-10-1 Revision 1, Brand Industrial Services, Inc. (Bisco), (August 12,1981).

8. J. R. Weeks, Anticipated Corrosion in the Vermont Yankee Spent Fuel Pool, Department of Applied Science, Brookhaven National Lab., Upton, New York, 13 p., (1977).

9. R. R. Burn, and G. Blessing, "Radiation Effects on Neutron Shielding Materials," Reactor Operating Experience, American Nuclear Society, Inc., La Grange Park, IL, pp. 48-49, (1979).

10. N. H. Macmillan and R. G. Naum, "The Behavior of B_4C Materials in Spent Fuel Storage Pools," pp. 288-89.

11. T. W. Evans, The Effects of Irradiation on Boron Carbide, Lit. Review, National Technical Information Service, U.S. Department of Commerce, Battelle-Northwest, Pacific Northwest Lab., Richland, Washington, 49 p., (1968).

12. R. A. Judd, Swelling of the Central Boral Divider Plate of an Irradiated Fuel Rod Shipping Basket, National Technical Information Service, U.S. Department of Commerce, Atomic Energy of Canada Ltd., Chalk River, Ontario, 20 p., (1968).

13. "Behavior of High-Density Spent-Fuel Storage Racks," Electric Power Research Institute, EPRI NP-4724, Project 2062-11, (August 1986).

14. L. J. Dietrick, Letter to author, 22 December 1986.

15. MURR Neutron Radiography Procedures, Missouri University Research Reactor, University of Missouri-Columbia, Columbia, Missouri, (1984).

16. P. Von Der Hardt and H. Rottger, editors, Neutron Radiography Handbook, Nuclear Science and Technology, (a commission of the European communities), D. Reidel Publishing Company, Boston, Mass., pp. 1-8, (1981).

17. L. E. Bryant, tech ed., and P. McIntire, ed., Radiography and Radiation Testing, vol. III of Nondestructive Testing Handbook, 2nd ed., American Society for Nondestructive Testing, United States, pp. 533-592, 187-238, 394-401, (1985).

18. D. R. Askeland, The Science and Engineering of Materials, Wadsworth, Inc., pp. 121-33, (1984).

19. R. J. Roark, Formulas for Stress and Strain, 4th ed., McGraw-Hill Book Company, St. Louis, MO, pp. 19, 31, and 79, (1965).

20. Modern Trends in Activation Analysis, Proc. of an Int. Conference, 19-22 April 1965, Texas A & M University, College Station, Texas, pp. 357- 362, (1965).

21. J. Spalek, "Total Neutron Cross Section," Argonne National Laboratory, A Manual of Reactor Laboratory Experiments, pp. 25.1-25.24.

22. J. W. Chastain, Jr., ed., U.S. Research Reactor Operation and Use, Addison-Wesley Publishing Company, Inc., Reading, Massachusetts, pp. 244, 250-51, (1958).

23. W. K. Foell, Small-Sample Reactivity Measurements in Nuclear Reactors, American Nuclear Society, Hinsdale, Illinois, pp. 13-38, (1972).

24. K. C. Ruzich, "Absorption Cross-Section Measurement by the Danger Coefficient Method," Argonne National Laboratory, A Manual of Reactor Laboratory Experiments, pp. 10.1-10.18.

VITA

Donald James Buth was born on August 26, 1963 in Washington, Missouri. He received his primary and secondary education in Union, Missouri. He has received his college education from East Central College, in Union, Missouri; and the University of Missouri-Rolla, in Rolla, Missouri. He received an Associate of Arts degree in Engineering from East Central College in Union, Missouri in July 1983; and a Bachelor of Science degree in Nuclear Engineering from the University of Missouri-Rolla, in July 1985.

He has been enrolled in the Graduate School of the University of Missouri-Rolla since August 1985 and has held the United State Department of the Interior Fellowship for the period August 1985 to December 1985, and the Power Fellowship for the period January 1986 to December 1986.

APPENDIX A

ORIGINAL LOCATION OF BORAFLEX^{TM} SAMPLES

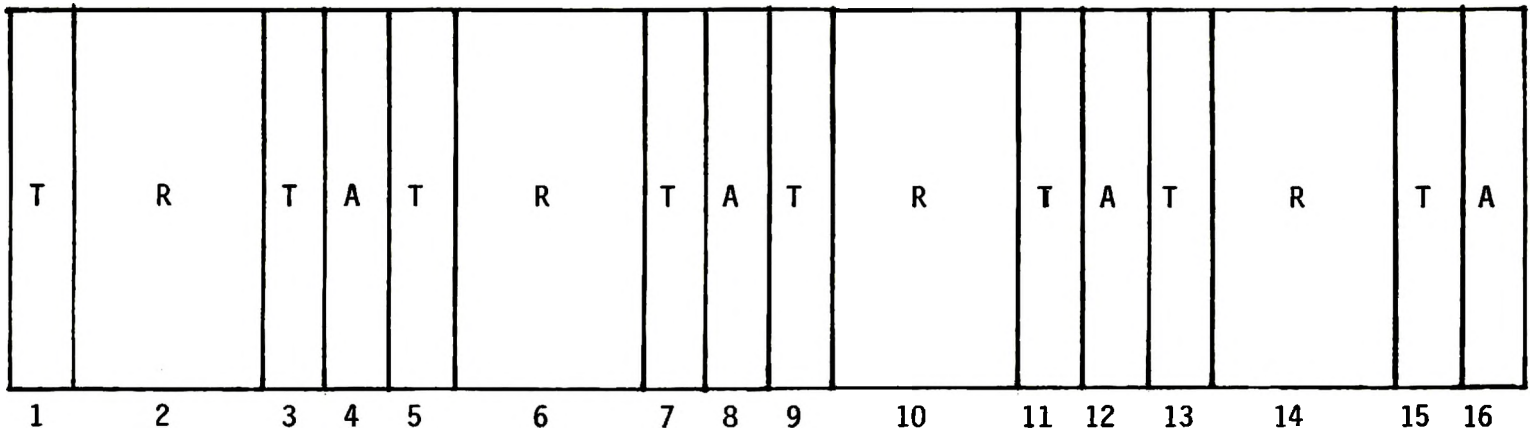

Figure A-1. Original Location of Boraflex™ Samples

A Attenuation Samples

R Radiography Samples

T Tensile Samples

APPENDIX B

RADIOGRAPH DATA

The following tables show the densities found at several locations on each radiograph, and the maximum discontinuity found. The specimen numbers with either a B or T are for the X-ray radiographs, and the plain numbers are for the neutron radiographs.

TABLE B-1

FILM DENSITY FOR SAMPLE SHEET 4

Specimen								Average Density
2B	0.52	0.58	0.56	0.56	0.54	0.58		0.57
2T	0.59	0.56	0.56	0.52	0.53			0.55
2	0.81	0.86	0.89	0.88	0.89	0.83	0.81	0.85
Maximum discontinuity found had a density of 0.75								

TABLE B-2

FILM DENSITY FOR SAMPLE SHEET 6

Specimen								Average
D	e	n	s	i	t	y		
6B	0.57	0.58	0.58	0.56	0.54			0.57
6T	0.54	0.55	0.57	0.60	0.58			0.57
6	0.92	0.85	1.00	0.92	0.84	0.83	0.83	
	0.86	0.80	0.98	0.96	0.85	0.85	0.80	0.88

No discontinuities were found.

TABLE B-3

FILM DENSITY FOR SAMPLE SHEET 10

Specimen								Average Density
10B	0.59	0.57	0.57	0.58	0.53			0.57
10T	0.57	0.56	0.59	0.53	0.52			0.55
10	0.83	0.83	0.82	0.84	0.80	0.80	0.83	0.82

No discontinuities were found.

TABLE B-4

FILM DENSITY FOR SAMPLE SHEET 14

Specimen								Average Density
14B	0.58	0.65	0.57	0.52	0.53			0.57
14T	0.56	0.55	0.58	0.56	0.55			0.56
14	0.86	0.89	0.94	0.95	0.89	0.82	0.84	0.88

Maximum discontinuity found had a density of 0.81

The penetrameters for the both the neutron and X-ray radiographs were made by slicing sections of Boraflex off of an end. These pieces were as uniform in thickness as possible, however, they may not have been uniform due to the state of the material they were cut from.

TABLE B-5

X-RAY PENETRAMETER DIMENSIONS AND DATA

Data			Average Density	Percent Thickness	True Thickness
0.88	0.87	0.87	0.87	91%	0.071
0.93	0.95	0.90	0.93	85%	0.066
1.12	1.23	1.16	1.17	70%	0.055
1.55	1.48	1.47	1.50	55%	0.043
2.04	1.96	1.78	1.93	40%	0.031
2.11	1.98	1.86	1.98	36%	0.028
1.26	1.27	1.25	1.26	46%	0.036
1.04	0.97	0.92	0.98	63%	0.049
0.81	0.83	0.81	0.82	77%	0.060
0.71	0.68	0.67	0.69	90%	0.070

TABLE B-6

NEUTRON PENETRAMETER DIMENSIONS AND DATA

Data		Average Density	Percent Thickness	True Thickness
1.25	1.20	1.22	64%	0.050
1.43	1.49	1.46	51%	0.040
2.16	2.17	2.17	26%	0.020

APPENDIX C

TENSILE TEST DATA

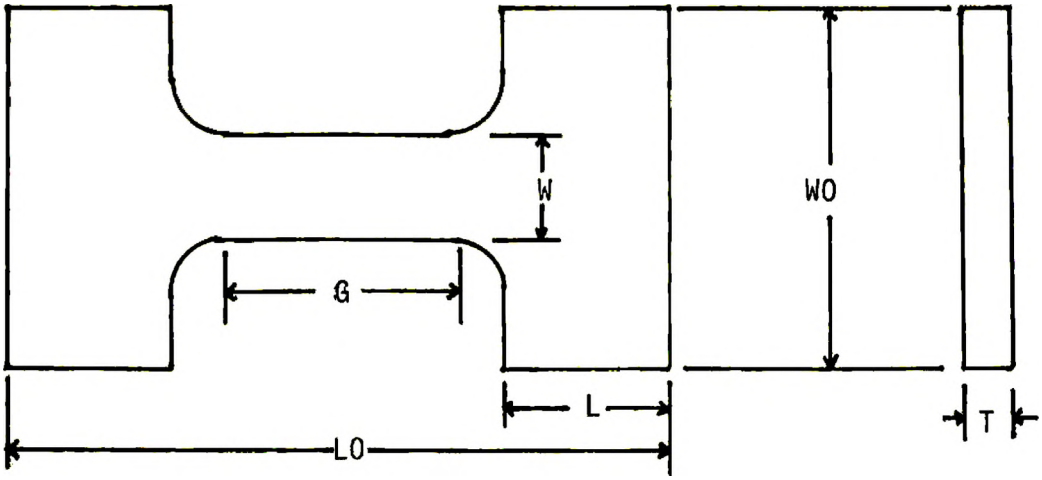

Figure C-1. Tensile Specimen Dimensions

L 5/8 ± 1/64 inch

LO 1½ ± 1/64 inch

T 11/128 ± 1/128 inch

W 3/16 ± 1/128 inch

WO 5/8 ± 1/64 inch

The following tables show the results of the tensile tests.

Tensile properties grouped by the specimen's horizontal location in the Boraflex sheet:

TABLE C-1

TENSILE PROPERTIES FOR STRAP 2

Initial Gage Length (in)	Final Gage Length (in)	Percent Elongation	Load at Rupture (lb)	Cross Sectional Area (in^2)	Stress At Failure (psi)
0.6250	0.9226	47.6	4.62	0.01611	2.87E+02
0.6250	0.8305	32.9	4.18	0.01611	2.59E+02
0.6250	0.8919	42.7	4.62	0.01611	2.87E+02
0.6250	0.9652	54.4	4.62	0.01611	2.87E+02
0.6250	0.9085	45.4	4.51	0.01611	2.80E+02
0.6250	0.9226	47.6	4.95	0.01611	3.07E+02
0.6250	1.0030	60.5	5.17	0.01611	3.21E+02
0.6250	0.7289	16.6	2.20	0.01273	1.73E+02
0.6250	0.7620	21.9	3.30	0.01273	2.59E+02
0.6250	0.7219	15.5	2.09	0.01273	1.64E+02
0.6250	0.7124	14.0	2.09	0.01273	1.64E+02

TABLE C-2

TENSILE PROPERTIES FOR STRAP 3

Initial Gage Length (in)	Final Gage Length (in)	Percent Elongation	Load at Rupture (lb)	Cross Sectional Area (in^2)	Stress At Failure (psi)
0.6250	0.9321	49.1	6.05	0.01611	3.75E+02
0.6250	0.9911	58.6	6.60	0.01611	4.10E+02
0.6250	0.9833	57.3	5.88	0.01611	3.65E+02
0.6250	0.9833	57.3	6.27	0.01611	3.89E+02
0.6250	1.0266	64.3	7.26	0.01611	4.51E+02
0.6250	1.0423	66.8	7.37	0.01611	4.57E+02
0.6250	0.9163	46.6	5.28	0.01611	3.28E+02
0.6250	0.6250	0.0	6.27	0.01611	3.89E+02
0.6250	1.0266	64.3	6.71	0.01611	4.16E+02
0.6250	1.0030	60.5	6.27	0.01611	3.89E+02
0.6250	0.9557	52.9	5.77	0.01611	3.58E+02
0.6250	0.9951	59.2	6.87	0.01611	4.27E+02
0.6250	0.9754	56.1	5.17	0.01611	3.21E+02

TABLE C-3

TENSILE PROPERTIES FOR STRAP 5

Initial Gage Length (in)	Final Gage Length (in)	Percent Elongation	Load at Rupture (lb)	Cross Sectional Area (in^2)	Stress At Failure (psi)
0.6250	0.9085	45.4	6.38	0.01611	3.96E+02
0.6250	0.9636	54.2	7.64	0.01611	4.74E+02
0.6250	1.0069	61.1	7.20	0.01611	4.47E+02
0.6250	1.0305	64.9	7.42	0.01611	4.61E+02
0.6250	0.9722	55.6	4.07	0.01611	2.53E+02
0.6250	0.9274	48.4	4.18	0.01611	2.59E+02
0.6250	0.7667	22.7	3.46	0.01273	2.72E+02
0.6250	0.7510	20.2	3.08	0.01273	2.42E+02
0.6250	0.8022	28.3	4.12	0.01273	3.24E+02
0.6250	0.7667	22.7	2.97	0.01273	2.33E+02

TABLE C-4

TENSILE PROPERTIES FOR STRAP 6

Initial Gage Length (in)	Final Gage Length (in)	Percent Elongation	Load at Rupture (lb)	Cross Sectional Area (in^2)	Stress At Failure (psi)
0.6250	0.9321	49.1	5.17	0.01611	3.21E+02
0.6250	0.9392	50.3	5.17	0.01611	3.21E+02
0.6250	0.9581	53.3	4.62	0.01611	2.87E+02
0.6250	0.9888	58.2	5.50	0.01611	3.41E+02
0.6250	0.9557	52.9	4.73	0.01611	2.94E+02
0.6250	0.7431	18.9	2.75	0.01273	2.16E+02
0.6250	0.7407	18.5	2.75	0.01273	2.16E+02
0.6250	0.7431	18.9	2.42	0.01273	1.90E+02
0.6250	0.7384	18.1	2.42	0.01273	1.90E+02

TABLE C-5

TENSILE PROPERTIES FOR STRAP 7

Initial Gage Length (in)	Final Gage Length (in)	Percent Elongation	Load at Rupture (lb)	Cross Sectional Area (in^2)	Stress At Failure (psi)
0.6250	0.9872	57.3	6.10	0.01611	3.79E+02
0.6250	1.0305	64.9	7.48	0.01611	4.64E+02
0.6250	1.0069	61.1	6.93	0.01611	4.30E+02
0.6250	1.0187	63.0	6.54	0.01611	4.06E+02
0.6250	0.9652	54.4	4.07	0.01611	2.53E+02
0.6250	0.7313	17.0	2.31	0.01273	1.81E+02
0.6250	0.7431	18.9	2.58	0.01273	2.03E+02
0.6250	0.7628	22.0	2.97	0.01273	2.33E+02
0.6250	0.7352	17.6	2.42	0.01273	1.90E+02

TABLE C-6

TENSILE PROPERTIES FOR STRAP 9

Initial Gage Length (in)	Final Gage Length (in)	Percent Elongation	Load at Rupture (lb)	Cross Sectional Area (in^2)	Stress At Failure (psi)
0.6250	0.9793	56.7	5.94	0.01611	3.69E+02
0.6250	1.0266	64.3	7.64	0.01611	4.74E+02
0.6250	0.9872	58.0	7.53	0.01611	4.68E+02
0.6250	1.0030	60.5	7.86	0.01611	4.88E+02
0.6250	0.9415	50.6	4.07	0.01611	2.53E+02
0.6250	0.9085	45.4	4.40	0.01611	2.73E+02
0.6250	0.7274	16.4	2.14	0.01273	1.69E+02
0.6250	0.7392	18.3	2.69	0.01273	4.10E+02
0.6250	0.7234	15.7	2.14	0.01273	1.69E+02
0.6250	0.7313	17.0	2.20	0.01273	1.73E+02

TABLE C-7

TENSILE PROPERTIES FOR STRAP 11

Initial Gage Length (in)	Final Gage Length (in)	Percent Elongation	Load at Rupture (lb)	Cross Sectional Area (in^2)	Stress At Failure (psi)
0.6250	2.1211	239.4	4.29	0.01611	2.66E+02
0.6250	0.9794	56.7	5.72	0.01611	3.55E+02
0.6250	0.9499	52.0	5.50	0.01611	3.41E+02
0.6250	0.9942	59.1	4.51	0.01611	2.80E+02
0.6250	0.9604	53.7	3.96	0.01611	2.46E+02
0.6250	0.9321	49.1	4.29	0.01611	2.66E+02
0.6250	0.7431	18.9	2.86	0.01273	2.25E+02
0.6250	0.7727	23.6	3.85	0.01273	3.02E+02
0.6250	0.8022	28.4	3.63	0.01273	2.85E+02
0.6250	0.7579	21.3	2.75	0.01273	2.16E+02

TABLE C-8

TENSILE PROPERTIES FOR STRAP 13

Initial Gage Length (in)	Final Gage Length (in)	Percent Elongation	Load at Rupture (lb)	Cross Sectional Area (in^2)	Stress At Failure (psi)
0.6250	0.9647	54.3	4.73	0.01611	2.94E+02
0.6250	0.9794	56.7	5.39	0.01611	3.35E+02
0.6250	0.9794	56.7	5.61	0.01611	.48E+02
0.6250	0.9499	52.0	5.72	0.01611	3.55E+02
0.6250	0.9499	52.0	5.61	0.01611	3.48E+02
0.6250	1.0030	60.5	4.07	0.01611	2.53E+02
0.6250	0.8494	35.9	4.51	0.01611	2.80E+02
0.6250	0.8896	42.3	4.40	0.01611	2.73E+02
0.6250	0.7431	18.9	2.42	0.01273	1.90E+02
0.6250	0.7431	18.9	2.64	0.01273	2.07E+02
0.6250	0.7727	23.6	3.41	0.01273	2.68E+02
0.6250	0.7727	23.6	3.74	0.01273	2.94E+02

TABLE C-9

TENSILE PROPERTIES FOR STRAP 15

Initial Gage Length (in)	Final Gage Length (in)	Percent Elongation	Load at Rupture (lb)	Cross Sectional Area (in^2)	Stress At Failure (psi)
0.6250	0.9647	54.3	4.51	0.01611	2.80E+02
0.6250	0.9647	54.3	5.06	0.01611	3.14E+02
0.6250	1.0090	61.4	5.28	0.01611	3.28E+02
0.6250	1.0090	61.4	4.84	0.01611	3.00E+02
0.6250	0.9368	49.9	3.74	0.01611	2.32E+02
0.6250	0.9392	50.3	4.29	0.01611	2.66E+02
0.6250	0.7431	18.9	2.64	0.01273	2.07E+02
0.6250	0.7727	23.6	3.41	0.01273	2.68E+02
0.6250	0.7727	23.6	2.86	0.01273	2.25E+02
0.6250	0.7727	23.6	2.86	0.01273	2.25E+02

Tensile properties grouped by the specimen's vertical location in the Boraflex sheet.

TABLE C-10

TENSILE PROPERTIES FOR STRAP SECTION A

Initial Gage Length (in)	Final Gage Length (in)	Percent Elongation	Load at Rupture (lb)	Cross Sectional Area (in^2)	Stress At Failure (psi)
0.6250	0.9226	47.6	4.62	0.01611	2.87E+02
0.6250	0.9321	49.1	2.86	0.01611	3.75E+02
0.6250	0.9911	58.6	3.41	0.01611	4.10E+02
0.6250	0.9163	46.6	5.28	0.01611	3.28E+02
0.6250	0.9085	45.4	6.38	0.01611	3.96E+02
0.6250	0.9321	49.1	5.17	0.01611	3.21E+02
0.6250	0.9872	58.0	6.10	0.01611	3.79E+02
0.6250	0.9793	56.7	5.94	0.01611	3.69E+02
0.6250	2.1211	239.4	4.29	0.01611	2.66E+02
0.6250	0.9647	54.3	4.73	0.01611	2.94E+02
0.6250	0.9647	54.3	4.51	0.01611	2.80E+02
0.6250	0.7289	16.6	2.20	0.01273	1.73E+02
0.6250	0.7667	22.7	3.46	0.01273	2.72E+02
0.6250	0.7431	18.9	2.75	0.01273	2.16E+02
0.6250	0.7313	17.0	2.31	0.01273	1.81E+02
0.6250	0.7274	16.4	2.14	0.01273	1.69E+02
0.6250	0.7274	16.4	2.09	0.01273	1.64E+02
0.6250	0.7431	18.9	2.86	0.01273	2.25E+02
0.6250	0.7431	18.9	2.42	0.01273	1.90E+02
0.6250	0.7431	18.9	2.64	0.01273	2.07E+02

TABLE C-11

TENSILE PROPERTIES FOR STRAP SECTION B

Initial Gage Length (in)	Final Gage Length (in)	Percent Elongation	Load at Rupture (lb)	Cross Sectional Area (in^2)	Stress At Failure (psi)
0.6250	0.8281	32.9	4.18	0.01611	2.59E+02
0.6250	1.0266	64.3	6.71	0.01611	4.16E+02
0.6250	0.9557	52.9	5.77	0.01611	3.58E+02
0.6250	0.9951	59.2	6.87	0.01611	4.27E+02
0.6250	0.9636	54.2	7.64	0.01611	.74E+02
0.6250	0.9392	50.3	5.17	0.01611	3.21E+02
0.6250	1.0305	64.9	7.48	0.01611	4.64E+02
0.6250	1.0266	64.3	7.64	0.01611	4.74E+02
0.6250	0.9794	56.7	5.72	0.01611	3.55E+02
0.6250	0.9794	56.7	5.39	0.01611	3.35E+02
0.6250	0.9647	54.3	5.06	0.01611	3.14E+02
0.6250	0.7620	21.9	3.30	0.01273	2.59E+02
0.6250	0.7510	20.2	3.08	0.01273	2.42E+02
0.6250	0.7407	18.5	2.75	0.01273	2.16E+02
0.6250	0.7431	18.9	2.58	0.01273	2.03E+02
0.6250	0.7392	18.3	2.69	0.01273	4.10E+02
0.6250	0.7727	23.6	3.85	0.01273	3.02E+02
0.6250	0.7431	18.9	2.64	0.01273	2.07E+02
0.6250	0.7727	23.6	3.41	0.01273	2.68E+02

TABLE C-12

TENSILE PROPERTIES FOR STRAP SECTION C

Initial Gage Length (in)	Final Gage Length (in)	Percent Elongation	Load at Rupture (lb)	Cross Sectional Area (in^2)	Stress At Failure (psi)
0.6250	0.8919	42.7	4.62	0.01611	2.87E+02
0.6250	0.9833	57.3	6.27	0.01611	3.89E+02
0.6250	1.0266	64.3	7.26	0.01611	4.51E+02
0.6250	0.6250	0.0	6.27	0.01611	3.89E+02
0.6250	0.9581	53.3	4.62	0.01611	2.87E+02
0.6250	1.0069	61.1	6.93	0.01611	4.30E+02
0.6250	1.0090	61.4	5.28	0.01611	3.28E+02
0.6250	0.9872	57.3	1.64	0.01611	3.89E+02
0.6250	1.0344	65.5	3.81	0.01611	2.36E+02
0.6250	0.8919	42.7	4.62	0.01611	2.87E+02
0.6250	1.0069	61.1	7.20	0.01611	4.47E+02
0.6250	0.9581	53.3	4.84	0.01611	2.87E+02
0.6250	1.0030	60.5	6.93	0.01611	4.30E+02
0.6250	0.9872	58.0	7.53	0.01611	4.68E+02
0.6250	0.9499	52.0	5.50	0.01611	3.41E+02
0.6250	0.9794	56.7	5.61	0.01611	3.48E+02
0.6250	1.0090	61.4	5.17	0.01611	3.21E+02
0.6250	0.7219	15.5	2.09	0.01273	1.64E+02
0.6250	0.8022	28.3	4.12	0.01273	3.24E+02
0.6250	0.7431	18.9	2.42	0.01273	1.90E+02
0.6250	0.7628	22.0	2.97	0.01273	2.33E+02
0.6250	0.7234	15.7	2.14	0.01273	1.69E+02
0.6250	0.8022	28.4	3.63	0.01273	2.85E+02
0.6250	0.7727	23.6	3.41	0.01273	2.68E+02
0.6250	0.7727	23.6	2.86	0.01273	2.25E+02

TABLE C-13

TENSILE PROPERTIES FOR STRAP SECTION D

Initial Gage Length (in)	Final Gage Length (in)	Percent Elongation	Load at Rupture (lb)	Cross Sectional Area (in^2)	Stress At Failure (psi)
0.6250	0.9652	54.4	4.62	0.01611	2.87E+02
0.6250	0.9833	57.3	5.88	0.01611	3.65E+02
0.6250	1.0423	66.8	7.37	0.01611	4.57E+02
0.6250	1.0030	60.5	6.27	0.01611	3.89E+02
0.6250	0.9754	56.1	5.17	0.01611	3.21E+02
0.6250	1.0305	64.9	7.42	0.01611	4.61E+02
0.6250	0.9888	58.2	5.50	0.01611	3.41E+02
0.6250	1.0187	63.0	6.54	0.01611	4.06E+02
0.6250	1.0030	60.5	7.86	0.01611	4.88E+02
0.6250	0.9942	59.1	4.51	0.01611	2.80E+02
0.6250	0.9499	52.0	5.72	0.01611	3.55E+02
0.6250	1.0090	61.4	4.84	0.01611	3.00E+02
0.6250	0.7124	14.0	2.09	0.01273	1.64E+02
0.6250	0.7667	22.7	2.97	0.01273	2.33E+02
0.6250	0.7384	18.1	2.42	0.01273	1.90E+02
0.6250	0.7352	17.6	2.42	0.01273	1.90E+02
0.6250	0.7313	17.0	2.20	0.01273	1.73E+02
0.6250	0.7579	21.3	2.75	0.01273	2.16E+02
0.6250	0.7727	23.6	3.74	0.01273	2.94E+02
0.6250	0.7727	23.6	2.86	0.01273	2.25E+02

TABLE C-14

TENSILE PROPERTIES FOR STRAP SECTION E

Initial Gage Length (in)	Final Gage Length (in)	Percent Elongation	Load at Rupture (lb)	Cross Sectional Area (in^2)	Stress At Failure (psi)
0.6250	0.9085	45.4	4.51	0.01611	2.80E+02
0.6250	0.9226	47.6	4.95	0.01611	3.07E+02
0.6250	1.0030	60.5	5.17	0.01611	3.21E+02
0.6250	0.9722	55.6	4.07	0.01611	2.53E+02
0.6250	0.9274	48.4	4.18	0.01611	2.59E+02
0.6250	0.9557	52.9	4.73	0.01611	2.94E+02
0.6250	0.9652	54.4	4.07	0.01611	2.53E+02
0.6250	0.9415	50.6	4.07	0.01611	2.53E+02
0.6250	0.9085	45.4	4.40	0.01611	2.73E+02
0.6250	0.9604	53.7	3.96	0.01611	2.46E+02
0.6250	0.9321	49.1	4.29	0.01611	2.66E+02
0.6250	1.0030	60.5	4.07	0.01611	2.53E+02
0.6250	0.8494	35.9	4.51	0.01611	2.80E+02
0.6250	0.8896	42.3	4.40	0.01611	2.73E+02
0.6250	0.9368	49.9	3.74	0.01611	2.32E+02
0.6250	0.9392	50.3	4.29	0.01611	2.66E+02

Tensile properties grouped by the angle from the normal direction of the Boraflex sheet.

TABLE C-15

TENSILE PROPERTIES FOR SPECIMEN AT 0 DEGREES

Initial Gage Length (in)	Final Gage Length (in)	Percent Elongation	Load at Rupture (lb)	Cross Sectional Area (in^2)	Stress At Failure (psi)
0.6250	0.9226	47.6	4.62	0.01611	2.87E+02
0.6250	0.9085	45.4	4.51	0.01611	2.80E+02
0.6250	0.9321	49.1	6.05	0.01611	3.75E+02
0.6250	0.9911	58.6	6.60	0.01611	4.10E+02
0.6250	0.9833	57.3	5.88	0.01611	3.65E+02
0.6250	0.9085	45.4	6.38	0.01611	3.96E+02
0.6250	0.9722	55.6	4.07	0.01611	2.53E+02
0.6250	0.9888	58.2	5.50	0.01611	3.41E+02
0.6250	0.9557	52.9	4.73	0.01611	2.94E+02
0.6250	1.0187	63.0	6.54	0.01611	4.06E+02
0.6250	0.9652	54.4	4.07	0.01611	2.53E+02
0.6250	0.9872	58.0	7.53	0.01611	4.68E+02
0.6250	0.9415	50.6	4.07	0.01611	2.53E+02
0.6250	0.9794	56.7	5.72	0.01611	3.55E+02
0.6250	0.9604	53.7	3.96	0.01611	2.46E+02
0.6250	0.9647	54.3	4.73	0.01611	2.94E+02
0.6250	1.0030	60.5	4.07	0.01611	2.53E+02
0.6250	1.0090	61.4	4.84	0.01611	3.00E+02
0.6250	0.9368	49.9	3.74	0.01611	2.32E+02

TABLE C-15 --CONTINUED

TENSILE PROPERTIES FOR SPECIMEN AT 0 DEGREES

Initial Gage Length (in)	Final Gage Length (in)	Percent Elongation	Load at Rupture (lb)	Cross Sectional Area (in^2)	Stress At Failure (psi)
0.6250	0.7289	16.6	2.20	0.01273	1.73E+02
0.6250	0.7667	22.7	3.46	0.01273	2.72E+02
0.6250	0.7384	18.1	2.42	0.01273	1.90E+02
0.6250	0.7352	17.6	2.42	0.01273	1.90E+02
0.6250	0.7234	15.7	2.14	0.01273	1.69E+02
0.6250	0.7727	23.6	3.85	0.01273	3.02E+02
0.6250	0.7431	18.9	2.42	0.01273	1.90E+02
0.6250	0.7727	23.6	2.86	0.01273	2.25E+02

TABLE C-16

TENSILE PROPERTIES FOR SPECIMEN AT 45 DEGREES

Initial Gage Length (in)	Final Gage Length (in)	Percent Elongation	Load at Rupture (lb)	Cross Sectional Area (in^2)	Stress At Failure (psi)
0.6250	0.8305	32.9	4.18	0.01611	2.59E+02
0.6250	0.9557	52.9	5.77	0.01611	3.58E+02
0.6250	0.9951	59.2	6.87	0.01611	4.27E+02
0.6250	0.9754	56.1	5.17	0.01611	3.21E+02
0.6250	1.0305	64.9	7.42	0.01611	4.61E+02
0.6250	0.9274	48.4	4.18	0.01611	2.59E+02
0.6250	0.9581	53.3	4.62	0.01611	2.87E+02
0.6250	1.0069	61.1	6.93	0.01611	4.30E+02
0.6250	1.0266	64.3	7.64	0.01611	4.74E+02
0.6250	0.9085	45.4	4.40	0.01611	2.73E+02
0.6250	2.1211	239.4	4.29	0.01611	2.66E+02
0.6250	0.9499	52.0	5.72	0.01611	3.55E+02
0.6250	0.8494	35.9	4.51	0.01611	2.80E+02
0.6250	0.8896	42.3	4.40	0.01611	2.73E+02
0.6250	1.0090	61.4	5.28	0.01611	3.28E+02
0.6250	0.7620	21.9	3.30	0.01273	2.59E+02
0.6250	0.7667	22.7	2.97	0.01273	2.33E+02
0.6250	0.7431	18.9	2.42	0.01273	1.90E+02
0.6250	0.7628	22.0	2.97	0.01273	2.33E+02
0.6250	0.7392	18.3	2.69	0.01273	4.10E+02
0.6250	0.7431	18.9	2.86	0.01273	2.25E+02
0.6250	0.7727	23.6	3.74	0.01273	2.94E+02
0.6250	0.7727	23.6	2.86	0.01273	2.25E+02

TABLE C-17

TENSILE PROPERTIES FOR SPECIMEN AT 90 DEGREES

Initial Gage Length (in)	Final Gage Length (in)	Percent Elongation	Load at Rupture (lb)	Cross Sectional Area (in^2)	Stress At Failure (psi)
0.6250	0.8919	42.7	4.62	0.01611	2.87E+02
0.6250	0.9226	47.6	4.95	0.01611	3.07E+02
0.6250	1.0030	60.5	5.17	0.01611	3.21E+02
0.6250	0.9163	46.6	5.28	0.01611	3.28E+02
0.6250	0.6250	0.0	6.27	0.01611	3.89E+02
0.6250	1.0266	64.3	6.71	0.01611	4.16E+02
0.6250	1.0030	60.5	6.27	0.01611	3.89E+02
0.6250	1.0069	61.6	7.20	0.01611	4.47E+02
0.6250	0.9392	50.3	5.17	0.01611	3.21E+02
0.6250	1.0305	64.9	7.48	0.01611	4.64E+02
0.6250	0.9793	56.7	5.94	0.01611	3.69E+02
0.6250	0.9942	59.1	4.51	0.01611	2.80E+02
0.6250	0.9321	49.1	4.29	0.01611	2.66E+02
0.6250	0.9499	52.0	4.62	0.01611	2.87E+02
0.6250	1.0090	61.4	4.95	0.01611	3.07E+02
0.6250	0.9392	50.3	4.29	0.01611	2.66E+02
0.6250	0.7219	15.5	2.09	0.01273	1.64E+02
0.6250	0.8022	28.3	4.12	0.01273	3.24E+02
0.6250	0.7407	18.5	2.75	0.01273	2.16E+02
0.6250	0.7431	18.9	2.58	0.01273	2.03E+02
0.6250	0.7274	16.4	2.14	0.01273	1.69E+02
0.6250	0.7579	21.3	2.75	0.01273	2.16E+02
0.6250	0.7727	23.6	3.41	0.01273	2.68E+02
0.6250	0.7727	23.6	3.41	0.01273	2.68E+02

TABLE C-18

TENSILE PROPERTIES FOR SPECIMEN AT 135 DEGREES

Initial Gage Length (in)	Final Gage Length (in)	Percent Elongation	Load at Rupture (lb)	Cross Sectional Area (in^2)	Stress At Failure (psi)
0.6250	0.9652	54.4	4.62	0.01611	2.87E+02
0.6250	0.9833	57.3	6.27	0.01611	3.89E+02
0.6250	1.0266	64.3	7.26	0.01611	4.51E+02
0.6250	1.0423	66.8	7.37	0.01611	4.57E+02
0.6250	0.9636	54.2	7.64	0.01611	4.74E+02
0.6250	0.9321	49.1	5.17	0.01611	3.21E+02
0.6250	0.9872	58.0	6.10	0.01611	3.79E+02
0.6250	1.0030	60.5	7.86	0.01611	4.88E+02
0.6250	0.9499	52.0	5.50	0.01611	3.41E+02
0.6250	0.9794	56.7	5.39	0.01611	3.35E+02
0.6250	0.9647	54.3	4.51	0.01611	2.80E+02
0.6250	0.7124	14.0	2.09	0.01273	1.64E+02
0.6250	0.7510	20.2	3.08	0.01273	2.42E+02
0.6250	0.7431	18.9	2.75	0.01273	2.16E+02
0.6250	0.7313	17.0	2.31	0.01273	1.81E+02
0.6250	0.7313	17.0	2.20	0.01273	1.73E+02
0.6250	0.8022	28.4	3.63	0.01273	2.85E+02
0.6250	0.7431	18.9	2.64	0.01273	2.07E+02
0.6250	0.7431	18.9	2.64	0.01273	2.07E+02

TABLE C-19

TENSILE PROPERTIES FOR SPECIMENS TESTED WITH LOAD CELL 1

Initial Gage Length (in)	Final Gage Length (in)	Percent Elongation	Load at Rupture (lb)	Cross Sectional Area (in^2)	Stress At Failure (psi)
0.6250	0.9321	49.1	2.86	0.01611	3.75E+02
0.6250	0.9911	58.6	3.41	0.01611	4.10E+02
0.6250	0.9833	57.3	5.88	0.01611	3.65E+02
0.6250	0.9833	57.3	6.27	0.01611	3.89E+02
0.6250	1.0266	64.3	7.26	0.01611	4.51E+02
0.6250	1.0423	66.8	7.37	0.01611	4.57E+02
0.6250	0.9163	46.6	5.28	0.01611	3.28E+02
0.6250	0.6250	0.0	6.27	0.01611	3.89E+02
0.6250	1.0266	64.3	6.71	0.01611	4.16E+02
0.6250	1.0030	60.5	6.27	0.01611	3.89E+02
0.6250	0.9557	52.9	5.77	0.01611	3.58E+02
0.6250	0.9951	59.2	6.87	0.01611	4.27E+02
0.6250	0.9754	56.1	5.17	0.01611	3.21E+02
0.6250	0.9085	45.4	6.38	0.01611	3.96E+02
0.6250	0.9636	54.2	7.64	0.01611	4.74E+02
0.6250	1.0069	61.1	7.20	0.01611	4.47E+02
0.6250	1.0305	64.9	7.42	0.01611	4.61E+02

TABLE C-19 --CONTINUED

TENSILE PROPERTIES FOR SPECIMENS TESTED WITH

LOAD CELL 1

Initial Gage Length (in)	Final Gage Length (in)	Percent Elongation	Load at Rupture (lb)	Cross Sectional Area (in^2)	Stress At Failure (psi)
0.6250	0.9872	58.0	6.10	0.01611	3.79E+02
0.6250	1.0305	64.9	7.48	0.01611	4.64E+02
0.6250	1.0069	61.1	6.93	0.01611	4.30E+02
0.6250	1.0187	63.0	6.54	0.01611	4.06E+02
0.6250	0.9793	56.7	5.94	0.01611	3.69E+02
0.6250	1.0266	64.3	7.64	0.01611	4.74E+02
0.6250	0.9872	58.0	7.53	0.01611	4.68E+02
0.6250	1.0030	60.5	7.86	0.01611	4.88E+02
0.6250	0.7667	22.7	3.46	0.01273	2.72E+02
0.6250	0.7510	20.2	3.08	0.01273	2.42E+02
0.6250	0.8022	28.3	4.12	0.01273	3.24E+02
0.6250	0.7667	22.7	2.97	0.01273	2.33E+02
0.6250	0.7313	17.0	2.31	0.01273	1.81E+02
0.6250	0.7431	18.9	2.58	0.01273	2.03E+02
0.6250	0.7628	22.0	2.97	0.01273	2.33E+02
0.6250	0.7352	17.6	2.42	0.01273	1.90E+02
0.6250	0.7274	16.4	2.14	0.01273	1.69E+02
0.6250	0.7392	18.3	2.69	0.01273	4.10E+02
0.6250	0.7234	15.7	2.14	0.01273	1.69E+02
0.6250	0.7313	17.0	2.20	0.01273	1.73E+02

TABLE C-20

TENSILE PROPERTIES FOR SPECIMENS TESTED WITH

LOAD CELL 2

Initial Gage Length (in)	Final Gage Length (in)	Percent Elongation	Load at Rupture (lb)	Cross Sectional Area (in^2)	Stress At Failure (psi)
0.6250	0.9226	47.6	4.62	0.01611	2.87E+02
0.6250	0.8305	32.9	4.18	0.01611	2.59E+02
0.6250	0.8919	42.7	4.62	0.01611	2.87E+02
0.6250	0.9652	54.4	4.62	0.01611	2.87E+02
0.6250	0.9085	45.4	4.51	0.01611	2.80E+02
0.6250	0.9226	47.6	4.95	0.01611	3.07E+02
0.6250	1.0030	60.5	5.17	0.01611	3.21E+02
0.6250	0.9722	55.6	4.07	0.01611	2.53E+02
0.6250	0.9274	48.4	4.18	0.01611	2.59E+02
0.6250	0.9321	49.1	5.17	0.01611	3.21E+02
0.6250	0.9392	50.3	5.17	0.01611	3.21E+02
0.6250	0.9581	53.3	4.62	0.01611	2.87E+02
0.6250	0.9557	52.9	4.73	0.01611	2.94E+02
0.6250	0.9888	58.2	5.50	0.01611	3.41E+02
0.6250	0.9652	54.4	4.07	0.01611	2.53E+02
0.6250	0.9415	50.6	4.07	0.01611	2.53E+02
0.6250	0.9085	45.4	4.40	0.01611	2.73E+02
0.6250	2.1211	239.4	4.29	0.01611	2.66E+02
0.6250	0.9794	56.7	5.72	0.01611	3.55E+02
0.6250	0.9499	52.0	5.50	0.01611	3.41E+02
0.6250	0.9942	59.1	4.51	0.01611	2.80E+02

TABLE C-20 --CONTINUED

TENSILE PROPERTIES FOR SPECIMENS TESTED WITH

LOAD CELL 2

Initial Gage Length (in)	Final Gage Length (in)	Percent Elongation	Load at Rupture (lb)	Cross Sectional Area (in^2)	Stress At Failure (psi)
0.6250	0.9604	53.7	3.96	0.01611	2.46E+02
0.6250	0.9321	49.1	4.29	0.01611	2.66E+02
0.6250	0.9647	54.3	4.73	0.01611	2.94E+02
0.6250	0.9794	56.7	5.39	0.01611	3.35E+02
0.6250	0.9794	56.7	5.61	0.01611	3.48E+02
0.6250	0.9499	52.0	5.72	0.01611	3.55E+02
0.6250	1.0030	60.5	4.07	0.01611	2.53E+02
0.6250	0.8494	35.9	4.51	0.01611	2.80E+02
0.6250	0.8896	42.3	4.40	0.01611	2.73E+02
0.6250	0.9647	54.3	4.51	0.01611	2.80E+02
0.6250	0.9647	54.3	5.06	0.01611	3.14E+02
0.6250	1.0090	61.4	5.28	0.01611	3.28E+02
0.6250	1.0090	61.4	4.84	0.01611	3.00E+02
0.6250	0.9368	49.9	3.74	0.01611	2.32E+02
0.6250	0.9392	50.3	4.29	0.01611	2.66E+02
0.6250	0.7289	16.6	2.20	0.01273	1.73E+02
0.6250	0.7620	21.9	3.30	0.01273	2.59E+02
0.6250	0.7219	15.5	2.09	0.01273	1.64E+02
0.6250	0.7124	14.0	2.09	0.01273	1.64E+02
0.6250	0.7431	18.9	2.75	0.01273	2.16E+02
0.6250	0.7407	18.5	2.75	0.01273	2.16E+02

TABLE C-20 --CONTINUED

TENSILE PROPERTIES FOR SPECIMENS TESTED WITH

LOAD CELL 2

Initial Gage Length (in)	Final Gage Length (in)	Percent Elongation	Load at Rupture (lb)	Cross Sectional Area (in^2)	Stress At Failure (psi)
0.6250	0.7431	18.9	2.42	0.01273	1.90E+02
0.6250	0.7384	18.1	2.42	0.01273	1.90E+02
0.6250	0.7431	18.9	2.86	0.01273	2.25E+02
0.6250	0.7727	23.6	3.85	0.01273	3.02E+02
0.6250	0.8022	28.4	3.63	0.01273	2.85E+02
0.6250	0.7579	21.3	2.75	0.01273	2.16E+02
0.6250	0.7431	18.9	2.42	0.01273	1.90E+02
0.6250	0.7431	18.9	2.64	0.01273	2.07E+02
0.6250	0.7727	23.6	3.41	0.01273	2.68E+02
0.6250	0.7727	23.6	3.74	0.01273	2.94E+02
0.6250	0.7431	18.9	2.64	0.01273	2.07E+02
0.6250	0.7727	23.6	3.41	0.01273	2.68E+02
0.6250	0.7727	23.6	2.86	0.01273	2.25E+02
0.6250	0.7727	23.6	2.86	0.01273	2.25E+02

TABLE C-21

TENSILE PROPERTIES FOR IRRADIATED SPECIMENS

Initial Gage Length (in)	Final Gage Length (in)	Percent Elongation	Load at Rupture (lb)	Cross Sectional Area (in^2)	Stress At Failure (psi)
0.6250	1.1368	81.9	2.20	0.01611	1.37E+02
0.6250	1.2077	93.2	2.64	0.01611	1.64E+02
0.6250	1.2156	94.5	2.42	0.01611	1.50E+02
0.6250	1.2234	95.7	2.53	0.01611	1.57E+02
0.6250	1.2116	93.9	2.20	0.01611	1.37E+02
0.6250	1.2313	97.0	2.20	0.01611	1.37E+02
0.6250	1.2392	98.3	2.42	0.01611	1.50E+02
0.6250	1.2156	94.5	2.31	0.01611	1.43E+02
0.6250	1.0502	68.0	1.76	0.01611	1.09E+02
0.6250	1.2156	94.5	2.42	0.01611	1.50E+02
0.6250	1.2116	93.9	2.42	0.01611	1.50E+02

APPENDIX D

TRACE ELEMENT ANALYSIS DATA

The following tables contain the data for the short term trace element analysis.

TABLE D-1

IDENTIFIED ISOTOPES FOR BORAFLEX™
FOR SHORT TERM ACTIVATION

Isotope	Concentration (uCi/g)		
Na-24	1.39E-1	±	4.29E-3
Mg-27	3.16E+0	±	1.56E-1
Cl-38	1.63E-1	±	1.96E-2
Ti-51	5.50E+0	±	8.59E-1
Mn-56	4.48E-1	±	3.00E-2
Zn-69m	4.22E-2	±	2.73E-3
Kr-87	8.94E+0	±	3.54E-1
Mo-101	2.14E+0	±	4.02E-1
In-116m	8.20E-1	±	7.82E-2
Eu-152m	1.08E-1	±	2.43E-2
Dy-165	2.93E-1	±	4.03E-2
Fe-59	4.70E-1	±	4.70E-2

Data for the long term trace element activation analysis.

TABLE D-2

IDENTIFIED ISOTOPES FOR BORAFLEX™
FOR LONG TERM ACTIVATION

Isotope	Concentration (uCi/g)		
Na-24	1.54E-1	±	8.24E-3
Sc-46	5.54E-4	±	2.26E-4
Fe-59	2.65E-3	±	3.57E-4
Zn-69m	1.39E+0	±	2.63E-2
As-76	8.61E-2	±	8.22E-3
Br-82	1.18E-2	±	2.26E-3
Sb-122	4.69E-3	±	1.06E-3
La-140	3.53E-2	±	1.32E-3
Sm-153	6.32E-2	±	2.05E-3
W-187	2.29E-1	±	4.57E-2

APPENDIX E

NEUTRON ATTENUATION DATA

Neutron attenuation data derived from the transmission method.

TABLE E-1

TOTAL THERMAL CROSS SECTION FOR BORAFLEX™

Thickness (inches)	Tranmission Coefficient	Macroscopic Cross section (cm^{-1})	Microscopic Cross section (barns)
2.203125E-01	4.61E-02	1.40E+01	1.85E-23
2.203125E-01	1.75E-02	1.84E+01	2.44E-23
2.203125E-01	1.83E-02	1.82E+01	2.41E-23
2.203125E-01	1.64E-02	1.87E+01	2.47E-23
2.203125E-01	1.91E-02	1.80E+01	2.39E-23
2.203125E-01	1.72E-02	1.84E+01	2.45E-23
2.203125E-01	1.30E-02	1.97E+01	2.62E-23
4.406250E-01	5.47E-02	6.59E+00	8.75E-24
4.406250E-01	7.10E-03	1.12E+01	1.49E-23
4.406250E-01	6.87E-03	1.13E+01	1.50E-23
4.406250E-01	2.74E-03	1.34E+01	1.78E-23
4.406250E-01	3.91E-03	1.26E+01	1.67E-23
6.609375E-01	4.90E-03	8.05E+00	1.07E-23
6.609375E-01	5.34E-03	7.92E+00	1.05E-23
6.609375E-01	7.01E-03	7.51E+00	9.96E-24
8.812500E-01	5.55E-03	5.89E+00	7.82E-24
8.812500E-01	5.21E-03	5.96E+00	7.92E-24
8.812500E-01	3.98E-03	6.27E+00	8.32E-24

TABLE E-2

TOTAL THERMAL NEUTRON CROSS SECTION FOR BORAL™

Thickness (inches)	Tranmission Coefficient	Macroscopic Cross section (cm^{-1})	Microscopic Cross section (barns)
2.500000E-01	8.83E-03	1.89E+01	2.40E-22
2.500000E-01	8.83E-03	1.89E+01	1.98E-22

TABLE E-3

TOTAL THERMAL NEUTRON CROSS SECTION FOR ALUMINUM

Thickness (inches)	Tranmission Coefficient	Macroscopic Cross section (cm^{-1})	Microscopic Cross section (barns)
2.500000E-01	9.24E-01	3.16E-01	5.25E-25
5.000000E-01	8.55E-01	3.13E-01	5.19E-25
7.500000E-01	8.15E-01	2.73E-01	4.53E-25

Neutron attenuation data derived from the danger coefficient method.

TABLE E-4

THERMAL ABSORPTION CROSS SECTION DATA FOR BORAFLEX™, AL-B-TEN™, AND CADMIUM

Material	Mass (mg)	Average Reg Rod Height	Reactivity Worth (% DeltaK/K)	Reactivity Change (% DeltaK/K)
None		14.0	0.2050	
Cadmium	0.8503	14.17	0.2092	0.0042
Boraflex™	0.5034	14.08	0.2070	0.0020
Al-B-Ten™	0.3120	14.02	0.2055	0.0005
None		14.00	0.2050	